

Preparation of hemp-based biocomposites and their potential industrial application

Lorenzo Gallina¹, Salah Chaji¹, Maela Manzoli¹, Fulvia Cravero², Chiara Gnoffo², Sebastia Gesti³, Alberto Frache^{2,*}, Giancarlo Cravotto^{1,*}

¹ Department of Drug Science and Technology, University of Turin, Via P. Giuria 9, 10125 Turin, Italy;

² Department of Applied Science and Technology, Politecnico di Torino, viale Teresa Michel 5, Alessandria, Italy

³ Novamont S.p.A., Via G. Fauser 8, Novara, Italy

Abstract

Biocomposites are an emerging field in plastic industry. The incorporation of agri-food waste in conventional or biobased polymer matrices allows the industry to lessen its carbon footprint, while producing recyclable plastic products. In this work, hemp hurd, a byproduct of hemp fibre production process, was used as a filler to prepare novel compostable composites in two different loadings (22% and 32% w/w respectively).

Waste hemp hurds were selected due to their abundance and the lack of derived high-value products. Three different polymers were used, namely poly[(tetramethyleneadipate)-co-(tetramethyleneterephthalate)] (PBAT) and poly(tetramethylene succinate) (PBS) as compostable polymers and a polyethylene elastomer for comparison. The bare polymers and prepared blends were then characterized for their structure and morphology by XRD and FESEM, as well as for their wettability, thermal and mechanical properties (namely energy absorbed on impact and flexural modulus). Structural and morphological characterization unveiled the different interactions occurring between hemp and the polymer matrices, suggesting the major impact of the type of used polymer when compared with biomass loading percentages. Mechanical tests showed that both PBAT and PBS blends properties are comparable to those of the pure polymers (i.e. in the case of PBAT the flexural modulus of the pure polymer was 82.2 MPa while the hemp-loaded blends stood at around 50 MPa, whereas all PBS polymers and blends were 220 MPa, with no statistical difference between samples). These biomaterials have also similar thermal properties with respect to the bare polymers, underlining the promising potential as sustainable alternative to pure polymers.

Highlights

- Waste hemp hurds were used to load biodegradable polymers at different percentages;
- Hemp hurd-based biomaterials with excellent properties were prepared;
- Polymer flexural behaviour was maintained even after hemp addition;
- Polymer-hemp interactions for each polymeric matrix were elucidated;
- Hemp substitutes up to 32% w/w of polymer without affecting its properties;

Keywords

biocomposites, hemp hurds, circular economy, waste valorisation

47

48 **1. Introduction**

49 In the emerging context of circular bioeconomy, the use of plant-derived resources for
50 developing novel biomaterials is gaining more interest for both academic and industrial
51 sectors. Keeping in mind that annual worldwide plastic production amounts to more than
52 460 million tons, 90% of which are from fossil sources¹, this trend will play a crucial role
53 in establishing sustainable waste management strategies and reducing the carbon footprint
54 linked to the plastic industry. In line with this approach, various countries and
55 international institutions have been taking actions to tackle plastic pollution. For instance,
56 the European Union started to address the plastic packaging waste management in 1994²
57 and redoubled its efforts in recent years, with initiatives such as the Zero Pollution Action
58 Plan³, for reducing the single use of plastics⁴, promoting viable biodegradable alternatives
59 and banning various microplastics-related applications^{5,6}.

60 Agricultural and agrifood-derived by-products are widely known to be cheap, abundant,
61 and renewable. The addition of this copious waste to degradable biopolymers can enhance
62 the sustainability properties of biomaterials, reduce the use of plastics, and contribute to
63 the valorisation of agrifood waste. This concept will further contribute to the valorisation
64 of biomasses for developing novel high-added value products, which can further be used
65 for plenty of industrial applications such as automotive, aeronautics, construction, food
66 packaging, interiors, among others. Various types of natural loading products, mainly
67 sisal, coir, jute, wood, cotton, palm, hemp, and bamboo, have been extensively
68 investigated and used for developing bio-based materials⁷⁻¹⁰. Among them, hemp bio-
69 composites are currently emerging as a promising field of research^{11,12}.

70 Italy stands as the 5th hemp (*Cannabis sativa* L.) producer in Europe and 10th in the world,
71 with nearly 5 million tons harvested yearly¹³. Hemp, also Known as “industrial hemp”,
72 refers to cannabis cultivars that are mainly grown for agricultural production (e.g., seeds,
73 fibres, oil and hurds). They are characterized by their low contents of the psychotropic
74 substance Δ -9 tetrahydrocannabinol (THC), typically less than 1%¹⁴. Hemp stem
75 processing is responsible for the generation of two materials, namely fibres and hurds.
76 The physico-chemical and mechanical characteristics of such bio-products make them
77 suitable candidates for application in various industrial sectors, in both forms. Hemp
78 fibres are usually used as reinforcing biomaterials to manufacture isolation mats to be
79 employed mainly in car interior panels and green buildings with thermoacoustic

80 insulation functions^{15,16}. Hurds, which constitute around 65% of total weight of hemp, are
81 widely used in hemp-lime products^{17,18}.

82 Along time, a considerable number of researchers have carried out studies aimed at
83 investigating the potential use of hemp fibres for developing novel bio-composites and
84 unlocking the effect of their loading on the characteristics of biomaterials. For example,
85 Pappua et al¹⁹. manufactured hybrid fibre reinforced eco-friendly materials using sisal
86 and hemp fibres with polylactic acid (PLA) employing melt processing and injection
87 moulding techniques. The reported findings revealed that the mechanical properties of
88 hybrid composites were improved compared to neat PLA. In a related note, Singh and
89 colleagues prepared hemp fibre composites, containing 10%, 20% and 30% hemp fibres
90 treated with 5% NaOH solution as reinforcement, and a mixture of virgin and recycled
91 high density polyethylene (HDPE) as matrix using injection moulding²⁰. Hemp fibre
92 reinforced polyethylene composites were compared with specimens made of 100% fresh
93 HDPE and mixture of virgin and recycled HDPE (50:50) in terms of tensile and flexural
94 properties. The study found that increasing the hemp content from 10 to 30% resulted in
95 a decline in the tensile strength of the hemp-based composite. The addition of hemp fibre
96 to composites made of HDPE was also investigated by Lu and Oza²¹. Bourmaud et al.²²
97 conducted a study on the use of recycled polymers, demonstrating the technical benefits
98 of using recycled materials instead of virgin ones. The study showed that recycled
99 polypropylene and recycled polypropylene/hemp fibre composite can exhibit good
100 mechanical properties after recycling.

101 Focusing the attention on hemp hurds, the available literature on their use is quite scarce
102 and their potential is not fully uncovered. However, hemp plastic bio-composites may
103 serve as a viable alternative to pure plastic or wood products for various industrial
104 applications. Loading hemp hurd into polymer matrices has been shown to impart good
105 mechanical, thermal, and acoustic properties to the resulting composite²³. Sassoni et al.¹⁸
106 reported a study on novel hemp-based composite materials designed for building
107 applications. These materials, produced by bonding hemp hurds with a novel hybrid
108 organic–inorganic binder, were characterized by both thermal insulation and physical-
109 mechanical resistance. Another study investigated the effect of simulated recycling of
110 HDPE up to six times and evaluated its suitability as a matrix for hemp hurd bio-
111 composites²⁴. The behaviour of the hemp plastic composites with less than 15% hemp

112 hurd powder resembled that of pure HDPE. However, when the composites contained
113 more than 15% of the powder, the particles began to aggregate, resulting in a deterioration
114 of properties. Further extensive information about hemp-based composites can be found
115 in various review papers^{12,16,25}.

116 The aim of the present work is to contribute to the valorisation of hemp hurds with the
117 goal of achieving zero agri-food waste and limiting the use of plastics in accordance with
118 the United Nations Sustainable Development Goals (SDGs). To do so, different
119 percentages of hemp hurds were used without any pretreatment to load different
120 polymers. The chosen polymers were poly[(tetramethyleneadipate)-co-
121 (tetramethyleneterephthalate)] (PBAT) and poly(tetramethylene succinate) (PBS) as
122 novel biomaterials and an ethylene-octene elastomer as a well known polymer for
123 comparison. The resulting materials were characterized after undergoing a pre-mixing
124 step followed by compression moulding to correlate their mechanical properties with their
125 structure and morphology.

126

127

128 **2. Materials and Methods**

129

130 **2.1. Reagents and materials**

131 Ethylene-octene elastomer (QUEO 0203, Borealis) was provided by GIMAC (Castronno,
132 VA, Italy). PBAT and PBS polymers were issued by Novamont S.p.A. (Novara, Italy).
133 PBS monomeric units are 1,4-butandiol and succinic acid, while PBAT is composed by
134 1,4-butandiol, adipic acid and terephthalic acid. Both PBS and PBAT are biodegradable
135 and compostable according to UNI EN 13432 norm. Prior to usage, PBAT was oven dried
136 overnight at 80°C in a laboratory oven.

137 Micronized hemp was provided by CHC-Chiaramonte Canapa Consapevole srls,
138 Belmonte Mezzagno (Palermo, Italy) and sieved to mesh 70 (212 µm).

139 Calcium carbonate (CaCO₃) was purchased from Merck (Merck KGaA, Darmstadt,
140 Germany). After sieving, hemp was dried at 45 °C in a laboratory oven upon reaching a
141 0.5 wt% moisture content and then stored in a tightly sealed container until usage.

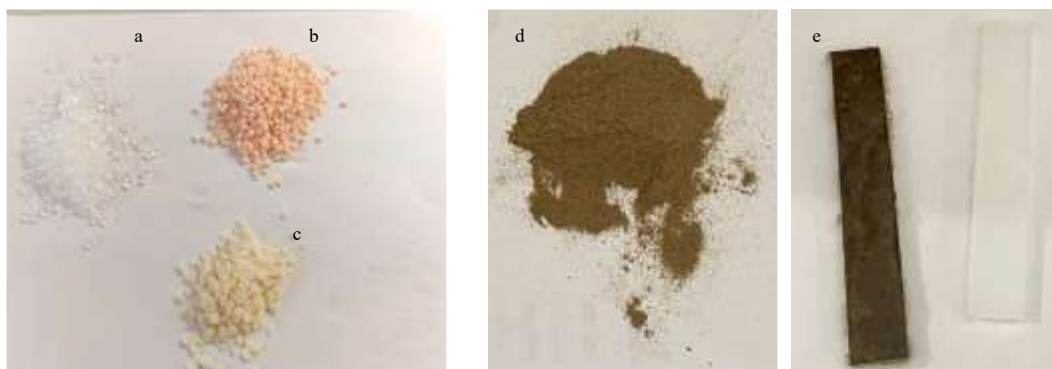
142

143 **2.2. Preparation of the samples**

144 Hemp – polymer blends were prepared by melt-mixing, using a Brabender W50E
145 apparatus (Plasti-Corder, Duisburg, Germany). The melting chamber was previously
146 heated to a specific temperature for each polymer (namely 135 °C for elastomer and 160
147 °C for both PBS and PBAT). A mixture of polymer, hemp and CaCO₃ (as a
148 compatibilizer) was poured in the melting chamber, and the components were allowed to
149 mix for 2 minutes at 50 rpm. Preliminary tests were conducted to find the optimal amounts
150 of hemp (based on visual and manual examination of the polymer after the mixing step,
151 excluding quantities that resulted in poor incorporation). For each polymer, three different
152 set of samples were prepared: pure polymer, polymer loaded with 22 wt% hemp and 5
153 wt% CaCO₃, and polymer loaded with 32 wt% hemp and 4,5 wt% CaCO₃ (all percentages
154 are calculated on weight).

155 The obtained blends were manually cut, so to be in the adequate size for the compression
156 molding and then compression-molded in a Collin P200T laboratory press (Maitenbeth,
157 Germany). Each polymer was pressed at the same temperature used for the blend
158 preparation for 3 minutes without applied pressure and then for 2 minutes with 50 bar
159 pressure for elastomer and 100 bar for PBS and PBAT. Following this procedure, plates
160 of the different blends were produced (**Figure 1**).

161



162

163 **Figure 1.** Polymer, hemp and prepared specimens. a) Elastomer; b) PBAT; c) PBS; d) micronized hemp;
164 e) loaded (left) and pure (right) elastomer.

165

166

167 **2.3. Morphological and structural characterization**

168 Field emission scanning electron microscopy (FESEM) measurements were carried out
169 using a TESCAN S9000G FESEM 3010 microscope (30 kV), equipped with a high

170 brightness Schottky emitter and Energy Dispersive X-ray Spectroscopy (EDS) analysis
171 thanks to a Ultim Max Silicon Drift Detector (SDD, Oxford, Abingdon-on-Thames, UK).
172 The samples were deposited on a stub that was coated with a conducting adhesive and
173 inserted into the chamber in a fully motorized procedure. The samples were submitted to
174 metallization with Cr (ca. 5 nm) to avoid any charging effect (Emitech K575X sputter
175 coater). Images were acquired by using both secondary electrons (SE) and backscattered
176 electrons (BSE) detectors. Both surface sides of the produced plates were analysed.
177 Images of the cross-sections of hemp-loaded polymer blends were acquired after breaking
178 the sample plates previously cooled by liquid nitrogen.
179 X-Ray Diffraction (XRD) patterns were collected by using a PW3050/60 X' Pert PRO
180 MPD diffractometer from PANalytical working in Bragg–Brentano geometry, using as a
181 source the high-powered ceramic tube PW3373/10 LFF with a Cu anode (Cu $K_{\alpha 1}$
182 radiation $\lambda = 1.5406 \text{ \AA}$) equipped with a Ni filter to attenuate K_{β} . Scattered photons were
183 collected by a real time multiple strip (RTMS) X' celerator detector. Data were collected
184 in the $5^{\circ} \leq 2\theta \leq 80^{\circ}$ angular range, with $0.02^{\circ} 2\theta$ steps.

185

186 **2.4. Rheology**

187 Rheological analyses were carried out with ARES TA Instrument rheometer (TA
188 Instruments Inc., New Castle, DE, USA). The instrument was equipped with a parallel
189 plate geometry having a diameter of 25 mm and a selected gap of 1 mm. The complex
190 viscosity was measured with frequency scans from 100 to 0,1 rad/s at constant strain
191 amplitude. The value was determined for each matrix by a strain sweep test, to fall in the
192 linear viscoelastic region. For all the materials the test was performed under inert
193 atmosphere.

194 The analysed samples were obtained with compression moulding and all the PBAT-based
195 materials were dried overnight at 80 °C in vacuum oven before the test. In addition, the
196 test's temperatures were properly selected. In particular, 135 °C for the elastomeric-based
197 materials and 160 °C for PBS and PBAT and corresponding hemp-filled.

198

199 **2.5. Contact angle**

200 Contact angle measurements were taken on a Attention Theta Lite (Biolin Scientific,
201 Västra Frölunda, Sweden) and data were elaborated by the OneAttention software on

202 Young-Laplace mode, with manual baseline correction. Instrument calibration was done
203 with a stainless steel 4.0003 mm ball. Each measure was taken with 4 μL water drop at
204 room temperature over 5 minutes observation, recording 0.51 FPS. Measurements were
205 done in triplicate.

206

207

208 **2.6. Thermal and mechanical properties**

209 Thermal analyses were performed using a Differential Scanning calorimeter (DSC) 7
210 system (Perkin-Elmer, Connecticut, USA). For calibration, indium standard samples were
211 used. Samples of 5–6 mg were weighed in aluminium pans and then heated at a rate of
212 10 $^{\circ}\text{C}/\text{min}$ in the 40–200 $^{\circ}\text{C}$ range under a nitrogen purge. An empty pan was used for
213 reference.

214 Three-point bending tests were performed according to ASTM International D790²⁶ on a
215 Instron 5966 machine (Instron, Norwood, MA, USA) equipped with a loading cell of 2
216 kN. Tests were carried out with a loading speed of 2 mm/min on 5mm radius supports
217 distanced 33 cm. The specimen was placed on the supports and the actuator applied a
218 force in the middle of the sample.

219 For each blend at least three specimens were used to obtain the Young modulus, and
220 average values with the corresponding standard deviation were calculated.

221 Impact tests were carried out accordingly to ASTM D4812²⁷ on a Zwick Roell HIT25P
222 (Zwick Roell Group, Ulm, Baden-Württemberg, Germany) equipped with a 5.4J
223 pendulum. Samples were loaded on the supports and the pendulum was manually
224 dropped. Unnotched samples were tested both at room temperature and, for specimens
225 that didn't break in the aforementioned conditions, after freezing in liquid nitrogen. Each
226 test was performed in triplicate and standard deviation was calculated.

227

228

229 **3. Results and discussion**

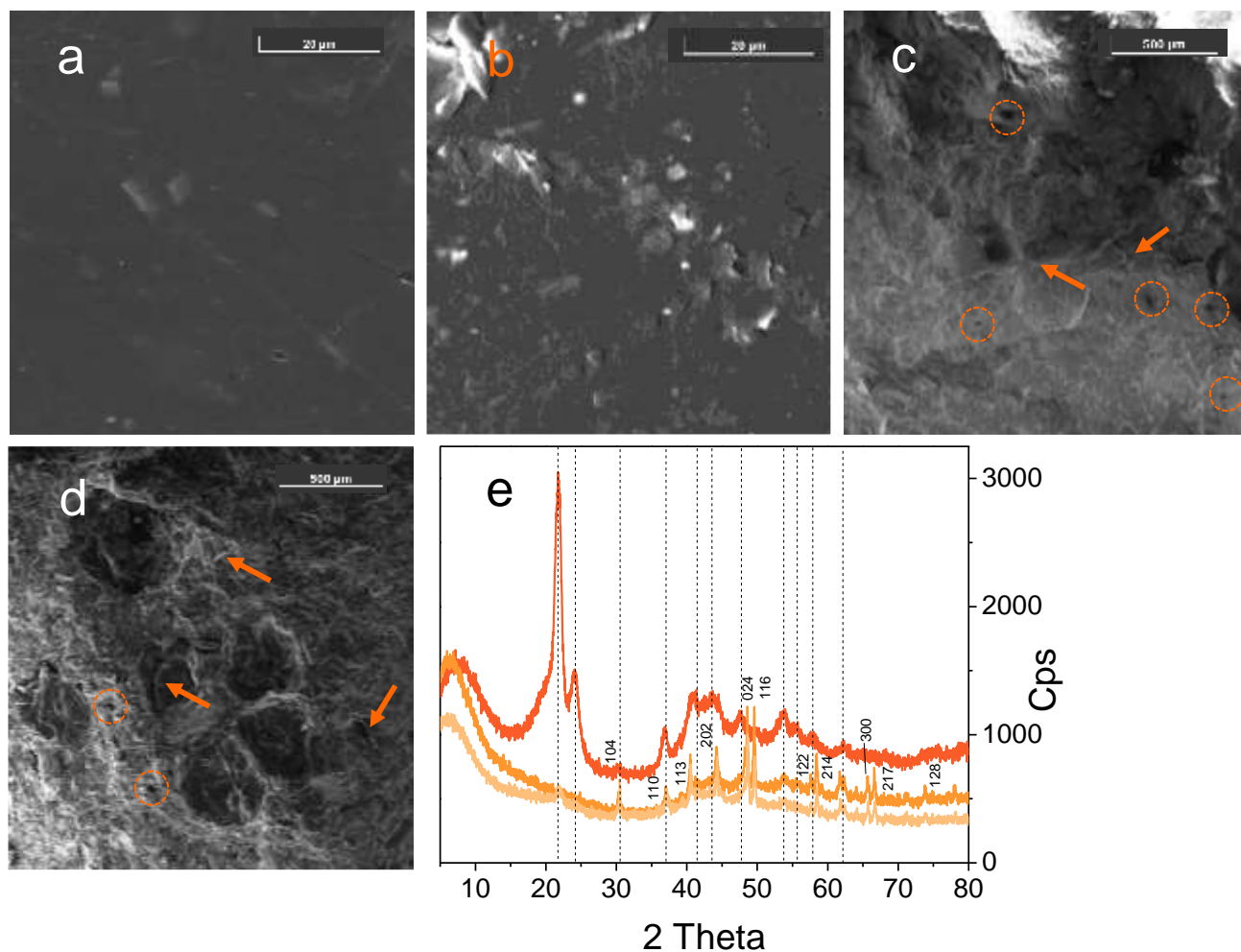
230

231 **3.1. Morphology and structure of the hemp–polymer blends**

232 FESEM measurements were carried out to investigate the morphology of the hemp–
233 polymer blends employed to obtain the bio-composites. Surfaces and cross-sections were

234 analysed to unravel the hemp spatial distribution within the polymeric matrix and
235 therefore to obtain information on the polymer-biomass interaction occurring within the
236 materials depending on the nature of the polymer. FESEM representative images
237 collected on the hemp-elastomer blends are shown in **Figure 2**. In particular, the surface
238 of these samples appears smooth, and some ridges are observed by increasing the hemp
239 loading from 22 wt% to 32 wt% (**Figure 2a** and **b**). Moreover, the presence of embedded
240 CaCO_3 observed as particles with squared shape and bright contrast for both elastomer-
241 hemp blends is confirmed by EDS mapping analysis (**Figure SI-1**). The FESEM
242 representative images collected on the cross-sections barely revealed the presence of few
243 hemp fibres (shown in **Figure SI-2** and signalled by arrows in **Figure 2c** and **d**) which
244 likely unthreaded from the polymer and slip off upon fractionation to obtain the cross-
245 sections, leaving small micrometric holes in their place (dashed circles). These features
246 indicate that hemp is dispersed within the elastomeric matrix and likely not strongly
247 interacting with the polymer.

248



249
 250
 251
 252
 253
 254
 255
 256
 257

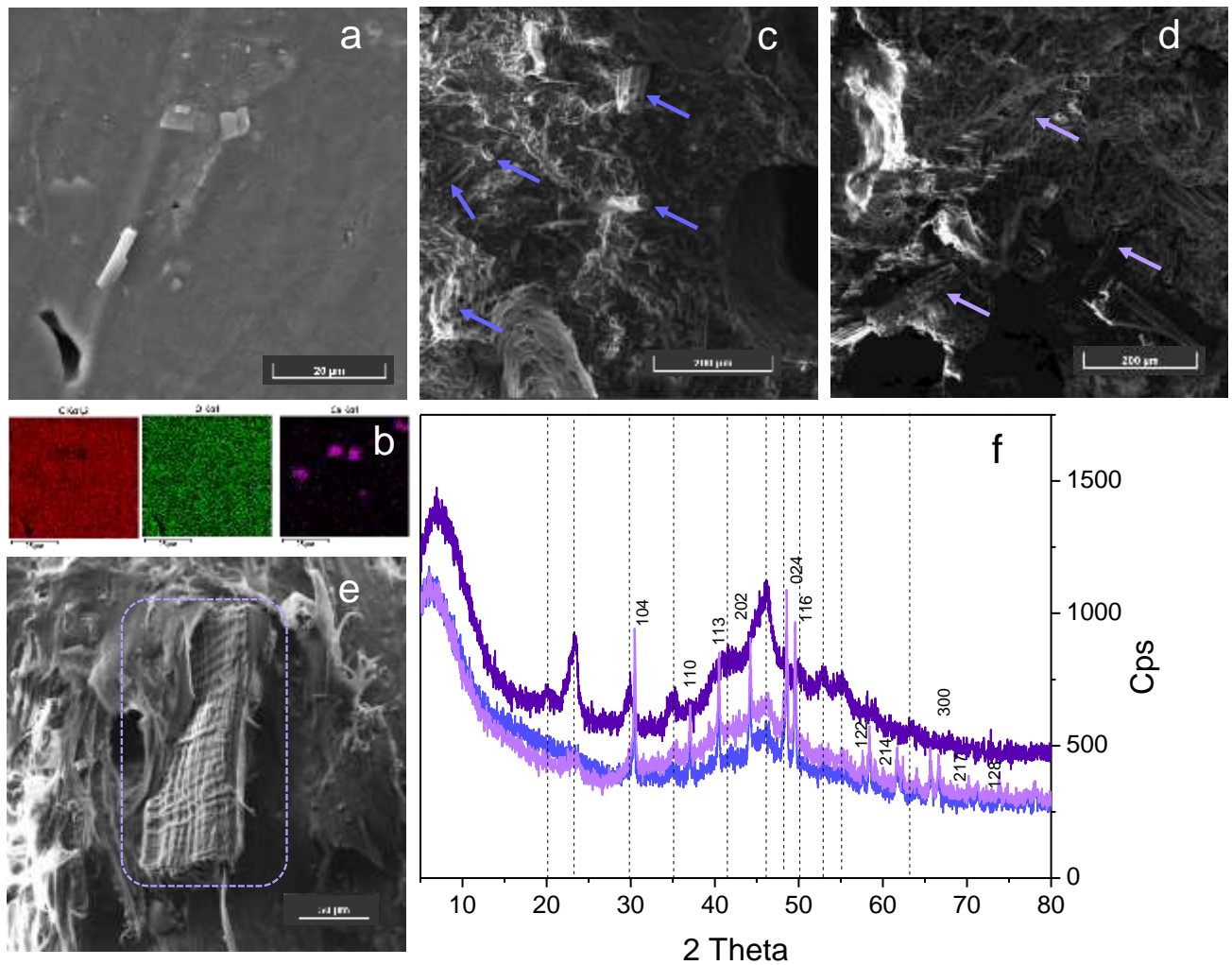
Figure 2. FESEM representative images of the hemp-polymer blends: surfaces of the bio-composite obtained from the elastomer loaded with 22 wt% (a) and 32 wt% hemp loading (b), cross section of the elastomer with 22 wt% (c) and 32 wt% hemp loading (d). Images taken with the SE detector at 15 keV. Instrumental magnification 4000 \times (a and b), 130000 \times (c and d). XRD patterns (e) of the bare elastomer (dark orange line), elastomer loaded with 22 wt% (orange line) and 32 wt% hemp loading (light orange line). Miller indexes for rhombohedral calcite crystalline phase (black, 00-002-0623). The position of the peaks of the elastomer is pointed out by dashed lines.

258 The XRD patterns of bare elastomer (dark orange line), elastomer loaded with 22 wt%
 259 (orange line) and 32 wt% hemp loading (light orange line) are shown in **Figure 2e**. The
 260 elastomer displays two characteristic peaks in the 20 $^{\circ}$ -25 $^{\circ}$ 2 θ range. When hemp is
 261 introduced in the blends, only a small peak at 2 θ around 37 $^{\circ}$ is maintained, although
 262 greatly diminished in intensity, while the other peaks completely disappeared indicating
 263 deep structural changes induced by the presence of hemp. The indexed peaks are related
 264 to rhombohedral CaCO₃ (00-002-0623, calcite). CaCO₃ and bare hemp were also
 265 analysed by XRD as reference samples. As expected, the XRD pattern of CaCO₃ shows
 266 sharp and intense peaks which are proper of a highly crystalline compound (**Figure SI-**

267 **3)**. These crystalline particles were observed in the FESEM images of the polymer blends,
268 thus confirming the findings from FESEM and EDS analyses which showed the inclusion
269 of inorganic particles inside the bio-composites. The XRD pattern of bare hemp reveals
270 instead the presence of a broad and structured peak in the 15°-25° 2Theta range typical
271 of both cellulose (00-003-0192) and amorphous lignin²⁸ components. Nevertheless, some
272 kind of structural order is further put in evidence by several peaks in the 15°-48° 2 Theta
273 range (15.3°, 21.9°, 24.8°, 27.0°, 28.5°, 29.7°, 30.5°, 36.3°, 38.5°, 40.1° and 47.5°), which
274 reveals that hemp is not completely amorphous (**Figure SI-4**).

275 When considering the bio-composites produced with the PBS polymer, quite different
276 features are observed. While elastomer/hemp surfaces appear smooth and flawless
277 (**Figure 2a and b**), the surface of the bio-composite containing PBS is jagged, irregular
278 and uneven (**Figure SI-5**), being however the morphology of the smooth regions quite
279 similar to that observed for the elastomer hemp bio-composite, independently from the
280 hemp loading (**Figure 3a**). First, by comparing the surfaces with the cross-sections, the
281 appearance of the holes located on the external surface greatly differs from that related to
282 the holes cross-sections. This feature allowed to ascribe the irregularities observed on the
283 surface of the PBS-containing blends to moulding-derived artifacts, as also supported by
284 the similar morphology of the bare PBS surface (**Figure SI-6**). The presence of protruding
285 parts made up by hemp fibres, which are intimately coated by the PBS polymer was
286 observed (**Figures 3c-e and Figure SI-6**). These fibres are reasonably formed during the
287 breaking of the sample plates at low temperature and demonstrates the occurrence of
288 polymer-biomass surface interactions. Such strong interaction could be attributed to the
289 formation of hydrogen bonds between cellulose-hemicellulose on hemp and the PBS
290 carbonyl groups. As a result, hemp fibres embedded in this polymer break simultaneously
291 with the matrix and remain in place without slipping off as shown in **Figures 3c-e**. The
292 XRD patterns of bare PBS and of the corresponding blends are shown in **Figure 3f**.
293 Similarly to the elastomer-hemp blends, the peaks at 2Theta around 25° is observed only
294 in the XRD pattern of the bare polymer (dark violet line).

295



296

297 **Figure 3.** FESEM representative images of the hemp-PBS blends: surface of the PBS-hemp bio-composite
 298 with 32 wt% hemp loading (a), EDS maps of the region shown in a) for C, O and Ca (b), cross sections of
 299 the bio-composite with 22 wt% (c and d) and 32 wt% hemp loading (e). Images taken with the SE detector
 300 at 15 keV. Instrumental magnification 4000 \times (a), 400 \times (c and d) and 1000 \times (e). XRD patterns (f) of bare
 301 PBS (dark violet line), PBS loaded with 22 wt% (violet line) and 32 wt% hemp loading (light violet line).
 302 Miller indexes for rhombohedral calcite crystalline phase (black, 00-002-0623). The position of the peaks
 303 of PBS is pointed out by dashed lines.
 304

305 However, other peaks proper of PBS as those one at 30 $^\circ$ and between 45 $^\circ$ -50 $^\circ$ are still
 306 present in the blend, although their intensity is lower with respect to that of pure PBS.
 307 Therefore, in this case hemp induced contained structural modification of the polymer.
 308 PBAT blends also exhibit smooth surfaces (**Figure 4a** and **b** and **Figure SI-8**) and the
 309 images collected on the cross-sections show protruding hemp fibres intimately embedded
 310 within the polymer (**Figures 4c-e**). Another particularity of these samples is the presence
 311 of hemp-void and hemp-rich areas, appearing with roundish shape and smoother surface
 312 (with respect to the other areas with higher rugosity) as those reported in **Figure 3c** and

313 e. This feature could be attributed to the nature of the employed polymer, being PBAT an
314 aliphatic-aromatic copolymer. It can be hypothesized that while butandiol and adipic acid
315 moieties, being mainly composed of carbon atoms with sp^3 hybridization, are less
316 constrained within the polymeric structure, the carbon atoms of terephthalic acid are all
317 hybridized sp^2 , meaning that they all lie on the same plane.

318 Thus, spatial orientation of the PBAT polymer chains could be influenced by both degree
319 of freedom and interaction among the aromatic rings of the terephthalic moieties, creating
320 hydrophobic pockets which cannot bind the hemicellulose and cellulose hydroxyl groups.
321 Conversely, the PBAT samples do not show any peaks of the original polymer after
322 blending, and the hemp loading seems to have no effect on the entity of structural changes.
323 Only signals typical of an amorphous nature can be observed. While hemp inclusion
324 slightly modifies the broad peak in the $25-60^\circ$ 2θ range, its shape is not modified,
325 and the blends seem to maintain the same amorphous character.

326 Therefore, the characterization by FESEM combined with EDS performed on the three
327 samples (**Figures 2-4**) reveal the absence of hemp on the surfaces of the blends,
328 independently from the hemp loading, whereas $CaCO_3$ crystals are randomly distributed.
329 The analysis of the cross-sections put in evidence some differences in hemp distribution,
330 depending on the nature of the polymer and likely resulting from different polymer-hemp
331 interaction.

332

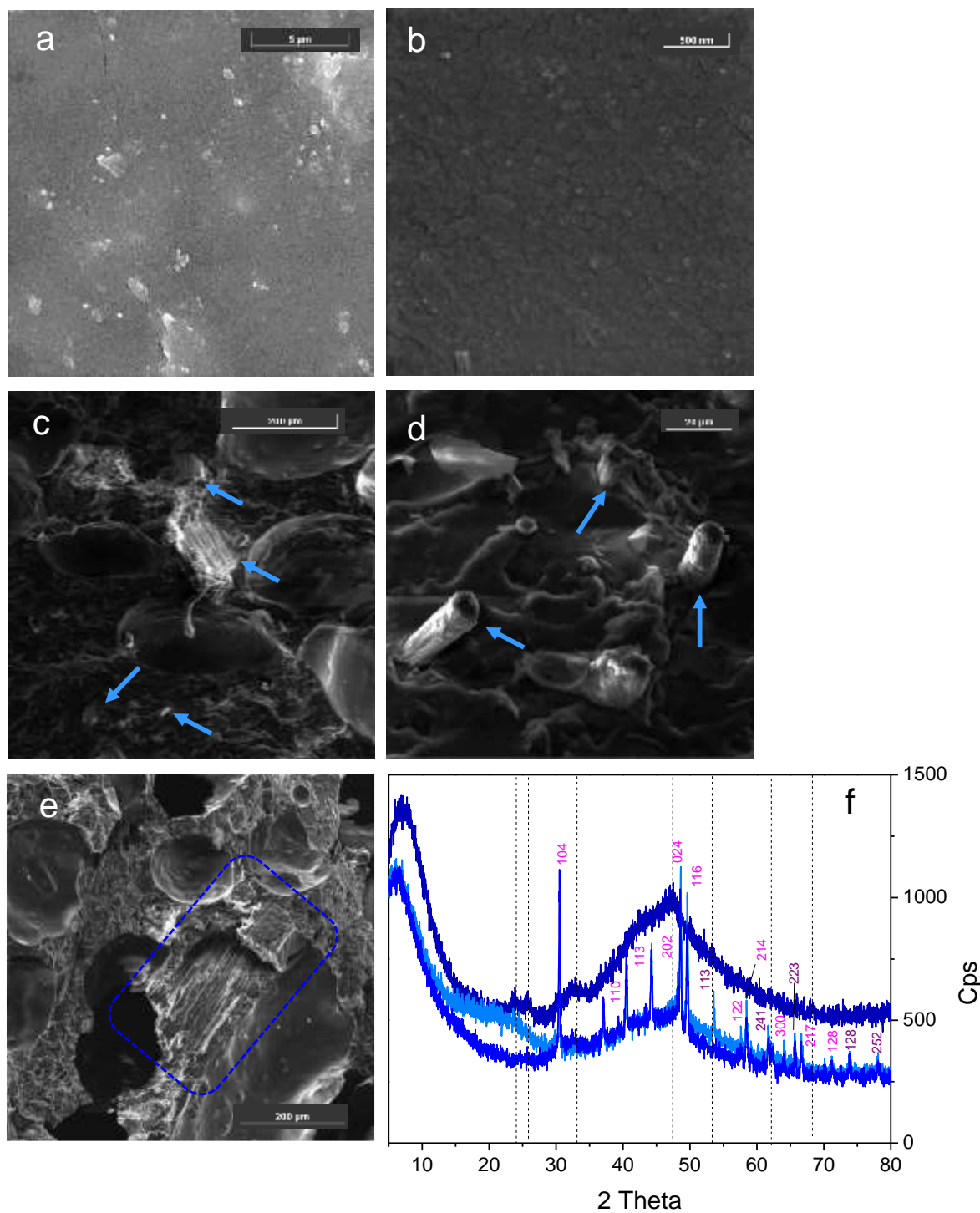
333

334

335

336

337



338

339

340

341

342

343

344

345

346

347

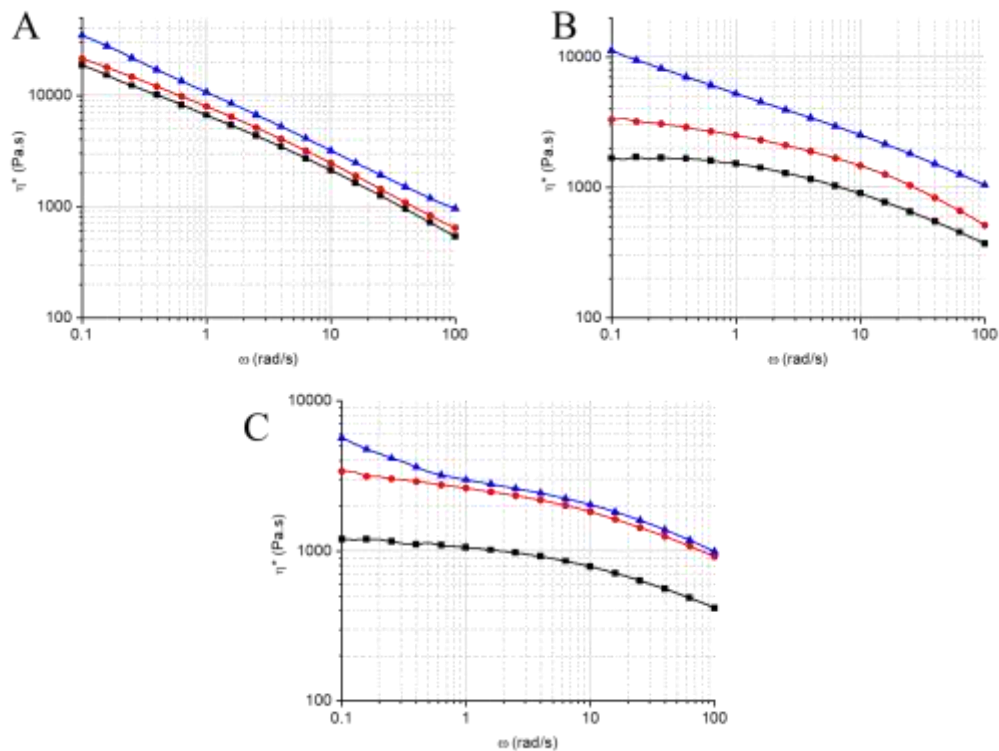
Figure 4. FESEM representative images of the hemp-PBAT blends: surfaces of the PBAT-hemp bio-composite with 22 wt% hemp loading (a and b), cross sections of the bio-composite with 22 wt% (c and d) and 32 wt% hemp loading (e). Images taken with the SE detector at 15 keV. Instrumental magnification 15000 \times (a), 100000 \times (b), 400 \times (c and e) and 2500 \times (d). XRD patterns (f) of bare PBAT (dark blue line), PBAT loaded with 22 wt% (blue line) and 32 wt% hemp loading (light blue line). Miller indexes for rhombohedral calcite crystalline phase (pink, 00-002-0623) and Miller indexes for orthorhombic aragonite crystalline phases (wine, 00-001-0628). The position of the peaks of PBS is pointed out by dashed lines.

348 **3.2. Rheological analysis**

349 Rheological analyses were carried out on all prepared composites and on pure polymers
350 for comparison (**Figure 5**). As reported in **Figure 5a**, the pure elastomer has a non-
351 Newtonian behaviour in all the frequency shift analysed. When considering the
352 composites, the one with 22 wt% of hemp has a rheological behaviour comparable to that
353 of the matrix. Thus, this hemp loading does not affect the rheological behaviour. On the
354 other hand, the composite containing 32 wt% hemp shows an increase of the viscosity in
355 all the frequency range. The increase in the complex viscosity is due to the addition of
356 hemp in the composite^{29,30}.

357 The complex viscosity of PBS is reported in **Figure 5b**. The matrix shows Newtonian
358 plateau at low frequencies, while at high values shear-thinning is appreciated. The
359 composite with 22 wt% hemp has a higher viscosity when compared to the matrix. Also
360 in this case, the Newtonian plateau and shear-thinning are observed at low and high
361 frequency respectively. Lastly, for the material containing 32 wt% of hemp the increase
362 of the viscosity in all the frequency range is observed, along with the disappearance of
363 the Newtonian plateau. Thus, the increase in the viscosity value is correlated to the hemp
364 content as expected from the literature^{31,32}. In addition, non-Newtonian behaviour
365 observed for the 32 wt% hemp load suggest the interaction of the filler with the
366 matrix^{32,33}.

367 **Figure 5c** refers to PBAT. For the matrix is observed the Newtonian plateau at low
368 frequencies and shear thinning at high frequencies. The introduction of 22 wt% of hemp
369 increases the viscosity along all the range of frequencies considered, and the Newtonian
370 plateau is appreciated at low values. The further increase in the hemp content does not
371 increase the viscosity in the mid-high frequency region, while the non-Newtonian
372 behaviour is appreciated at low values. The increase in the complex viscosity is related to
373 the presence of the hemp^{24,34}. In addition, also the non-Newtonian behaviour is due to the
374 filler^{24,35}.



375

376

377 **Figure 5.** Rheological behaviour of pure polymers and blends. Black lines represent pure polymers, red
 378 lines are for 22% hemp loading and blue lines refer to 32% hemp loading. a) Elastomer; b) PBS; c) PBAT.

379

380

3.3. Wettability

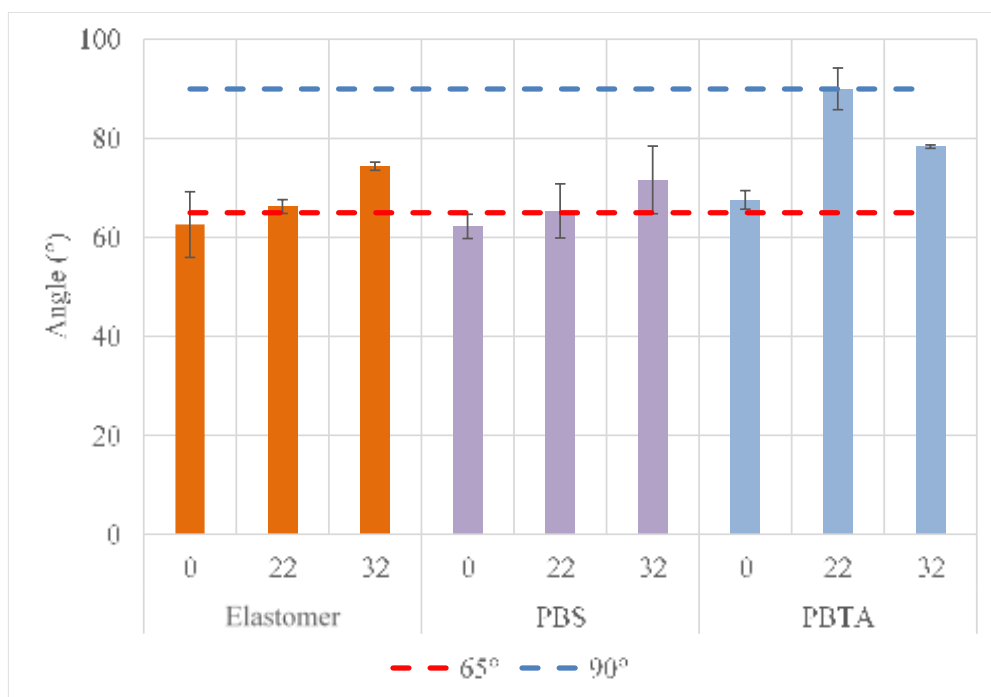
381 Polymers and blends wettability have been evaluated through contact angle measurement
 382 and the results are shown in **Figure 6**.

383 Elastomer samples show a statistically significant difference only for the 32 wt% hemp
 384 loading, while the pure polymer and 22 wt% hemp loaded one have the same behaviour.

385 Both loaded polymers could be considered hydrophobic by the standards of Vogler³⁶,
 386 while for the pure polymer much caution is needed regarding its possible hydrophobicity.

387 PBS shows no statistically significant difference for all treated samples, showing a clear
 388 hydrophobic behaviour only for 32 wt% loaded blend.

389



390 **Figure 6.** Contact angle for the different polymer blends. Numbers above polymer names specify the hemp
 391 loading. Green and red dashed lines show the commonly recognized hydrophobicity thresholds for
 392 polymers^{36,37}.
 393

394

395 By the same standards, both pure PBAT and its blends can be considered hydrophobic,
 396 and their behaviour is significantly changed by hemp addition.

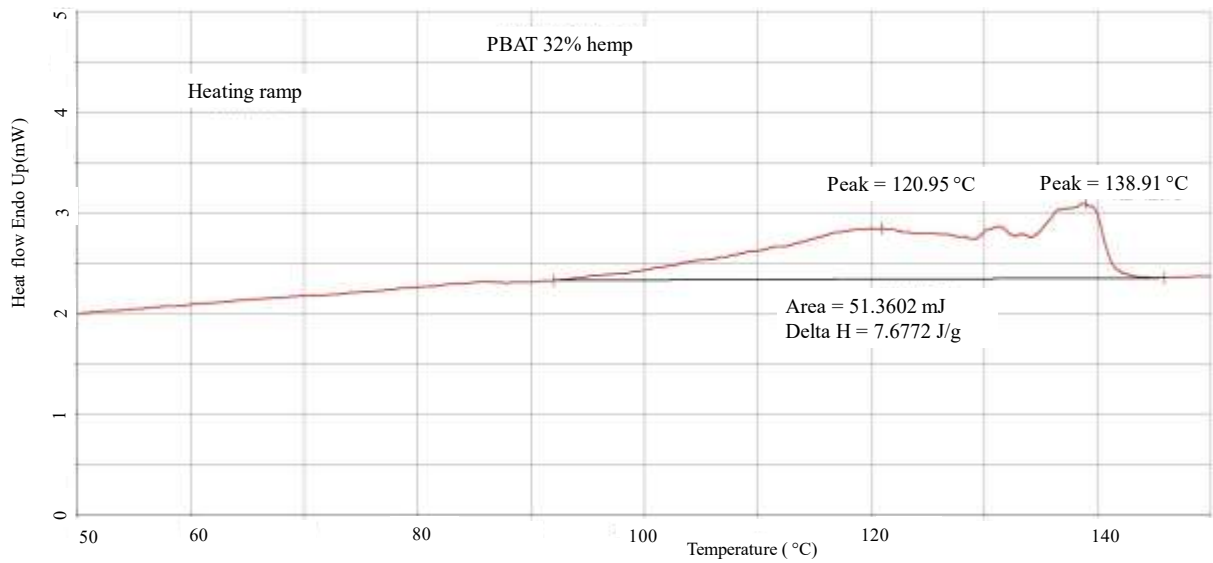
397 While there are significant differences between some samples, these variations don't
 398 fundamentally change the actual polymers behaviour and their destination of use. So,
 399 while PBAT can be considered for water-resisting coating or similar usage, much caution
 400 should be exercised with the other tested samples.

401

402 **3.4. Thermal analysis**

403 Calorimetric analyses were conducted on both pure polymers and blends. The amorphous
 404 nature of PBAT, as signalled by XRD (**Figure 4f**), has been further confirmed by the wide
 405 peaks observed in the DSC measurements. The irregular shape of the peaks may be
 406 attributed to a heterogeneous crystal habit formation due to polymer chains spatial
 407 constraints and high filler amount (**Figure 7**).

408



409

410 **Figure 7.** DSC thermogram of PBAT loaded with 32% hemp.

411

412 Elastomer and PBS instead present clear peaks. The results are summarized in **Table 1**

413 and DSC thermograms can be found in **Figure SI-9-16**.

414

415 **Table 1.** ΔH_f and peak melting temperatures of studied polymers in DSC.

Polymer	Hemp Loading (wt%)	ΔH_f (J/g)	Peak T (°C)
Elastomer	0	30.6	102.5
	22	68.53	97.2
	32	58.34	96.9
PBS	0	64.7	114.0
	22	52.0	112.0
	32	54.0	110.7
PBAT	0	16.6	117.4
	22	7.2	120.7
	32	<11.3	120.9; 138.9

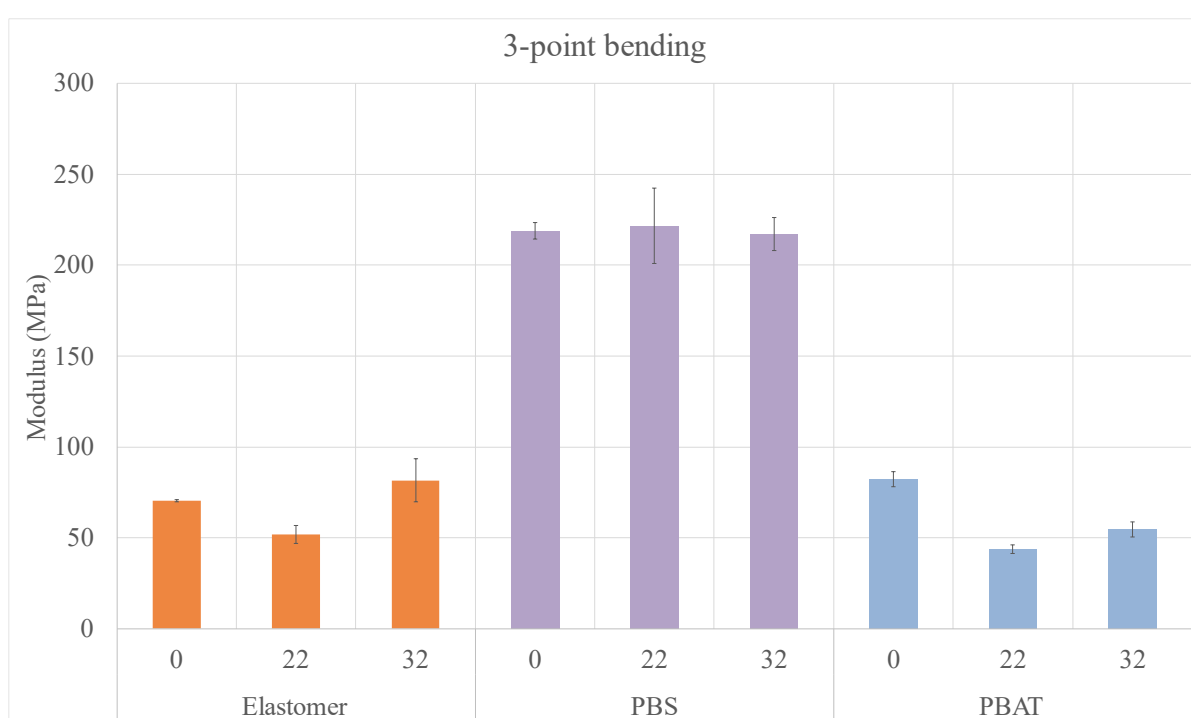
416

417

418 3.5. Mechanical properties

419 Samples mechanical properties have been investigated both for their resistance to impact
420 and flexural behaviour. Samples were subjected to a 3-point bending test and their
421 modulus was thus determined, as shown in **Figure 8**, which reports the values of flexural
422 modulus for pristine matrixes and composites with the highest percentage of hemp
423 content, equal to 32 wt %. It should be noted that the polymers were not broken under
424 common test conditions.

425



426

427 **Figure 8.** Modulus value for tested polymers and blends. Numbers above polymer names specify the hemp
428 loading.

429

430

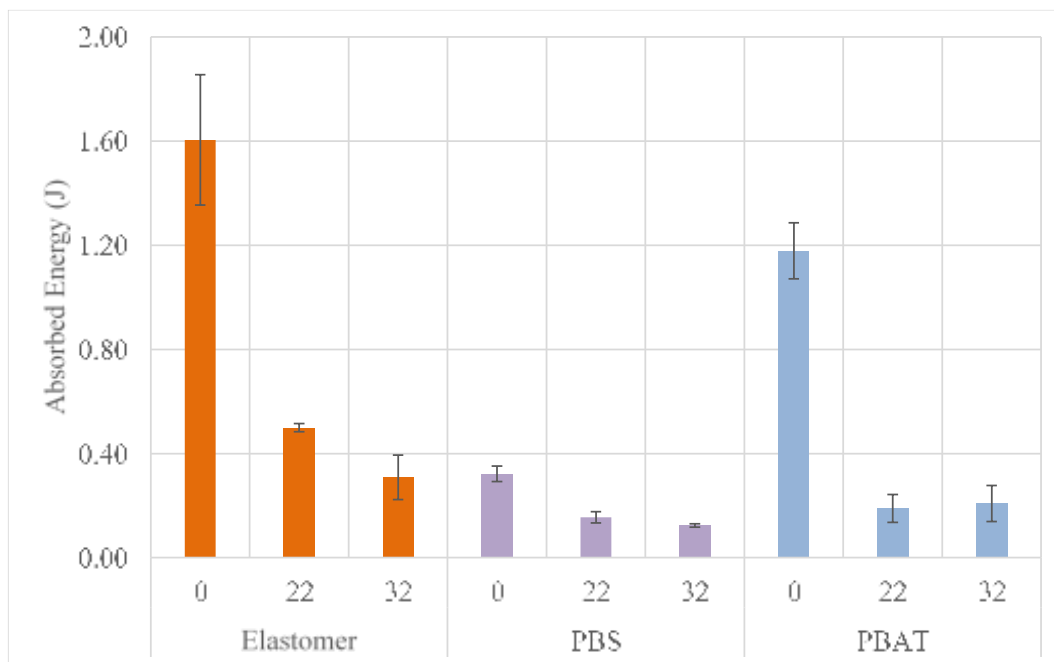
431 The flexural modulus mildly increases thanks to the presence of hemp only in the case of
432 the elastomer, while it remains almost constant for PBS and slightly diminishes for PBAT
433 (**Figure 8**).

434 In literature, the improvement of mechanical characteristics related to presence of hemp
435 into an elastomeric matrix is well-known³⁸⁻⁴¹. On the contrary, PBS shows no statistically
436 difference between pristine polymer and the hemp loaded one, while the reduction of the
437 flexural modulus for PBAT is likely to be related to the decreasing of this property with

438 high fibre content, in particular with loading beyond a certain value due to particle
439 agglomeration⁴²⁻⁴⁴. The most interesting finding is that the hemp addition to polymer
440 matrices does not fundamentally change their behaviour: variations are on a small scale
441 and the modulus maintains the same order of magnitude, meaning that hemp inclusion
442 does not affect meaningfully the flexural behaviour of the tested polymers.

443 Impact test results are shown in **Figure 9**. All the polymers only yielded when frozen in
444 liquid nitrogen.

445



446

447

448

449

Figure 9. Impact test results for pure polymers and loaded samples. Numbers above polymer names specify the hemp loading.

450

451

452

453

454

455

All systems show a statistically significant difference between the pure polymer and the loaded one and higher loadings lead to lower absorbed energy. In particular, all matrixes show diminishing absorbed energy with increasing presence of hemp. As in flexural test results, the most important finding regards the order of impact resistance of tested samples: hemp inclusion change the fundamental behaviour of these matrixes, that is strengthened by the filler presence.

456

457

458

459

Hemp has a huge effect on impact strength values of elastomer⁴⁰ and the ones of PBAT, which are considerably reduced^{33,44,45}, while PBS shows slightly reduction of impact strength when hemp is present⁴⁶ and the differences of this mechanical characteristic between 22 wt% and 32 wt% is little^{47,48}. In fact, several authors highlighted the decrease

460 of this mechanical property with increasing filler content when dealing with
461 biodegradable matrixes^{33,44,49}, as well as the reduction of impact strength for the
462 toughening of the overall composite^{45,49,50}.

463

464 **4. Conclusions**

465

466 In this study, one of the most abundant hemp byproducts, hemp hurds, was successfully
467 blended with different polymeric matrices for preparing biobased composites. The
468 preparation of such systems and complete structural, morphological, thermal and
469 mechanical characterization were described. The detailed morphological (FESEM) and
470 structural (XRD) characterization of the blends highlighted different polymer-hemp
471 interactions depending on the nature of the polymer rather than the tested hemp loadings.
472 Furthermore, mechanical analysis showed that hemp inclusion can maintain the
473 fundamental properties of the materials in terms of both bending and impact tests, since
474 the tested blends exhibited values within the same order of magnitude of pure polymers.
475 PBAT systems with elastomeric behaviour compared with an elastomeric PE and PBS
476 with stiffer behaviour were investigated. Interestingly, introducing up to 32 wt% waste
477 biomass in the polymer did not significantly change the mechanical properties: flexural
478 modulus of PBAT blends and pure polymer was 82.2 MPa for the pure polymer and
479 around 50 MPa for both the 22 wt% and 32 wt wt% hemp-loaded blends, a small
480 difference that doesn't change the common applications of this material, while no
481 statistically significant difference was found between all tested PBS polymers and blends,
482 which modulus stood at 220 MPa.

483 The proposed methodology in this work can greatly contribute to establishing a circular
484 economy concept in the hemp industry, while reducing the carbon footprint in materials
485 manufacturing processes. Furthermore, considering that two compostable polymers were
486 used in this study, the developed biomaterials offer a cost-effective solution for plastic
487 industries to partially replace polymers with agri-food byproducts while maintaining their
488 main characteristics.

489 Following this process, other agri-food waste products can be investigated for
490 incorporation into polymer matrices, advancing research into compostable, natural fibres-
491 based blends and their industrial applications.

492

493 **REFERENCES**

- 494 1. *International Energy Agency, The Future of Petrochemicals.*
495 <https://www.iea.org/reports/the-future-of-petrochemicals>. Published in 2018.
496 Accessed on 20 May 2024.
- 497 2. *European Parliament and Council Directive 94/62/EC on Packaging and*
498 *Packaging Waste.*; 1994.
- 499 3. *Communication from the Commission to the European Parliament, the Council, the*
500 *European Economic and Social Committee and the Committee of the Regions*
501 *Pathway to a Healthy Planet for All EU Action Plan: “Towards Zero Pollution for*
502 *Air, Water and Soil.”* Vol COM/2021/400 final.; 2021.
- 503 4. *Directive (EU) 2019/ of the European Parliament and of the Council of 5 June 2019*
504 *on the Reduction of the Impact of Certain Plastic Products on the Environment.*;
505 2019.
- 506 5. *Commission Regulation (EU) 2023/2055 Amending Annex XVII to Regulation (EC)*
507 *No 1907/2006 of the European Parliament and of the Council Concerning the*
508 *Registration, Evaluation, Authorisation and Restriction of Chemicals (REACH) as*
509 *Regards Synthetic Polymer Microparticles.*; 2023.
- 510 6. *Annex to the Commission Regulation (EU) 2023/2055 Amending Annex XVII to*
511 *Regulation (EC) No 1907/2006 of the European Parliament and of the Council*
512 *Concerning the Registration, Evaluation, Authorisation and Restriction of*
513 *Chemicals (REACH) as Regards Synthetic Polymer Microparticles.*; 2023.
- 514 7. Senthilkumar K, Saba N, Rajini N, et al. Mechanical properties evaluation of sisal
515 fibre reinforced polymer composites: A review. *Constr Build Mater.* 2018;174:713-
516 729. doi:10.1016/j.conbuildmat.2018.04.143
- 517 8. Pappu A, Patil V, Jain S, Mahindrakar A, Haque R, Thakur VK. Advances in
518 industrial prospective of cellulosic macromolecules enriched banana biofibre
519 resources: A review. *Int J Biol Macromol.* 2015;79:449-458.
520 doi:10.1016/j.ijbiomac.2015.05.013
- 521 9. Pickering KL, Efendy MGA, Le TM. A review of recent developments in natural
522 fibre composites and their mechanical performance. *Compos Part Appl Sci Manuf.*
523 2016;83:98-112. doi:10.1016/j.compositesa.2015.08.038
- 524 10. Thakur VK, Singha AS. Mechanical and Water Absorption Properties of Natural
525 Fibers/Polymer Biocomposites. *Polym-Plast Technol Eng.* 2010;49(7):694-700.
526 doi:10.1080/03602551003682067
- 527 11. Saradava BJ, Kathwadia AJ, Goraviyala AD, Joshi VK. Mechanical
528 characterization of hemp fiber reinforced polyester composites. 2016;1(5).
- 529 12. Moscariello C, Matassa S, Esposito G, Papiro S. From residue to resource: The
530 multifaceted environmental and bioeconomy potential of industrial hemp (Cannabis

- 531 sativa L.). *Resour Conserv Recycl.* 2021;175:105864.
532 doi:10.1016/j.resconrec.2021.105864
- 533 13. FAOstat data on 2022 world hemp production. FAOstat. Accessed March 12, 2024.
534 <https://www.fao.org/faostat/en/#data/QCL>
- 535 14. Johnson R. *Hemp as an Agricultural Commodity*. U.S. Congressional Research
536 Service; 2014. <https://crsreports.congress.gov/product/pdf/RL/RL32725>
- 537 15. Li Z, Wang L, Wang X. Compressive and flexural properties of hemp fiber
538 reinforced concrete. *Fibers Polym.* 2004;5(3):187-197. doi:10.1007/BF02902998
- 539 16. Ingrao C, Lo Giudice A, Bacenetti J, et al. Energy and environmental assessment of
540 industrial hemp for building applications: A review. *Renew Sustain Energy Rev.*
541 2015;51:29-42. doi:10.1016/j.rser.2015.06.002
- 542 17. Ip K, Miller A. Life cycle greenhouse gas emissions of hemp–lime wall
543 constructions in the UK. *Resour Conserv Recycl.* 2012;69:1-9.
544 doi:10.1016/j.resconrec.2012.09.001
- 545 18. Sassoni E, Manzi S, Motori A, Montecchi M, Canti M. Novel sustainable hemp-
546 based composites for application in the building industry: Physical, thermal and
547 mechanical characterization. *Energy Build.* 2014;77:219-226.
548 doi:10.1016/j.enbuild.2014.03.033
- 549 19. Pappu A, Pickering KL, Thakur VK. Manufacturing and characterization of
550 sustainable hybrid composites using sisal and hemp fibres as reinforcement of poly
551 (lactic acid) via injection moulding. *Ind Crops Prod.* 2019;137:260-269.
552 doi:10.1016/j.indcrop.2019.05.040
- 553 20. Singh S, Deepak D, Aggarwal L, Gupta VK. Tensile and Flexural Behavior of
554 Hemp Fiber Reinforced Virgin-recycled HDPE Matrix Composites. *Procedia Mater
555 Sci.* 2014;6:1696-1702. doi:10.1016/j.mspro.2014.07.155
- 556 21. Lu N, Oza S. Thermal stability and thermo-mechanical properties of hemp-high
557 density polyethylene composites: Effect of two different chemical modifications.
558 *Compos Part B Eng.* 2013;44(1):484-490. doi:10.1016/j.compositesb.2012.03.024
- 559 22. Bourmaud A, Le Duigou A, Baley C. What is the technical and environmental
560 interest in reusing a recycled polypropylene–hemp fibre composite? *Polym Degrad
561 Stab.* 2011;96(10):1732-1739. doi:10.1016/j.polymdegradstab.2011.08.003
- 562 23. Stevulova N, Kidalova L, Cigasova J, Junak J, Sicakova A, Terpakova E.
563 Lightweight Composites Containing Hemp Hurds. *Procedia Eng.* 2013;65:69-74.
564 doi:10.1016/j.proeng.2013.09.013
- 565 24. Jubinville D, Sharifi J, Fayazfar H, Mekonnen TH. Hemp hurd filled PLA - PBAT
566 blend biocomposites compatible with additive manufacturing processes:
567 Fabrication, rheology, and material property investigations. *Polym Compos.*
568 2023;44(12):8946-8961. doi:10.1002/pc.27749

- 569 25. Müssig J, Amaducci S, Bourmaud A, Beaugrand J, Shah DU. Transdisciplinary top-
570 down review of hemp fibre composites: From an advanced product design to crop
571 variety selection. *Compos Part C Open Access*. 2020;2:100010.
572 doi:10.1016/j.jcomc.2020.100010
- 573 26. *Standard Test Methods for Flexural Properties of Unreinforced and Reinforced*
574 *Plastics and Electrical Insulating Materials*. ASTM International
- 575 27. D20 Committee. *Standard Test Method for Unnotched Cantilever Beam Impact*
576 *Resistance of Plastics*. ASTM International [https://www.astm.org/d4812-](https://www.astm.org/d4812-19e01.html)
577 [19e01.html](https://www.astm.org/d4812-19e01.html)
- 578 28. Gomide RAC, De Oliveira ACS, Rodrigues DAC, et al. Development and
579 Characterization of Lignin Microparticles for Physical and Antioxidant
580 Enhancement of Biodegradable Polymers. *J Polym Environ*. 2020;28(4):1326-1334.
581 doi:10.1007/s10924-020-01685-z
- 582 29. DiKmen Küçük S, Tozluoğlu A, Güner Y, Arslan R, Sertkaya S. Nano-fibrillenmiş
583 selüloz / EPDM kompozitlerin mekanik, reolojik ve yaşlanma özellikleri. *Artvin*
584 *Çoruh Üniversitesi Orman Fakültesi Derg*. 2022;23(1):11-22.
585 doi:10.17474/artvinofd.934238
- 586 30. Miedzianowska J, Masłowski M, Strzelec K. Thermoplastic Elastomeric
587 Composites Filled with Lignocellulose Bioadditives. Part 1: Morphology,
588 Processing, Thermal and Rheological Properties. *Materials*. 2020;13(7):1598.
589 doi:10.3390/ma13071598
- 590 31. Arabeche K, Abdelmalek F, Delbreilh L, Zair L, Berrayah A. Physical and
591 rheological properties of biodegradable poly(butylene succinate)/Alfa fiber
592 composites. *J Thermoplast Compos Mater*. 2022;35(10):1709-1727.
593 doi:10.1177/0892705720904098
- 594 32. Bhattacharjee SK, Chakraborty G, Kashyap SP, Gupta R, Katiyar V. Study of the
595 Thermal, Mechanical and Melt Rheological Properties of Rice Straw Filled Poly
596 (Butylene Succinate) Bio-composites Through Reactive Extrusion Process. *J Polym*
597 *Environ*. 2021;29(5):1477-1488. doi:10.1007/s10924-020-01973-8
- 598 33. Yan Y, Dou Q. Effect of Peroxide on Compatibility, Microstructure, Rheology,
599 Crystallization, and Mechanical Properties of PBS/Waxy Starch Composites. *Starch*
600 *- Stärke*. 2021;73(3-4):2000184. doi:10.1002/star.202000184
- 601 34. Gupta A, Lolic L, Mekonnen TH. Reactive extrusion of highly filled,
602 compatibilized, and sustainable PHBV/PBAT – Hemp residue biocomposite.
603 *Compos Part Appl Sci Manuf*. 2022;156:106885.
604 doi:10.1016/j.compositesa.2022.106885
- 605 35. Mohammadi M, Heuzey MC, Carreau PJ, Taguet A. Morphological and
606 Rheological Properties of PLA, PBAT, and PLA/PBAT Blend Nanocomposites
607 Containing CNCs. *Nanomaterials*. 2021;11(4):857. doi:10.3390/nano11040857

- 608 36. Vogler EA. Structure and reactivity of water at biomaterial surfaces. *Adv Colloid*
609 *Interface Sci.* 1998;74(1-3):69-117. doi:10.1016/S0001-8686(97)00040-7
- 610 37. Law KY. Definitions for Hydrophilicity, Hydrophobicity, and Superhydrophobicity:
611 Getting the Basics Right. *J Phys Chem Lett.* 2014;5(4):686-688.
612 doi:10.1021/jz402762h
- 613 38. Stelescu MD, Airinei A, Barga A, et al. Mechanical Properties and Equilibrium
614 Swelling Characteristics of Some Polymer Composites Based on Ethylene
615 Propylene Diene Terpolymer (EPDM) Reinforced with Hemp Fibers. *Materials.*
616 2022;15(19):6838. doi:10.3390/ma15196838
- 617 39. Tutek K, Masek A. Hemp and Its Derivatives as a Universal Industrial Raw
618 Material (with Particular Emphasis on the Polymer Industry)—A Review.
619 *Materials.* 2022;15(7):2565. doi:10.3390/ma15072565
- 620 40. Wang J, Wu W, Wang W, Zhang J. Preparation and characterization of hemp hurd
621 powder filled SBR and EPDM elastomers. *J Polym Res.* 2011;18(5):1023-1032.
622 doi:10.1007/s10965-010-9503-4
- 623 41. Stelescu MD, Manaila E, Georgescu M, Nituica M. New Materials Based on
624 Ethylene Propylene Diene Terpolymer and Hemp Fibers Obtained by Green
625 Reactive Processing. *Materials.* 2020;13(9):2067. doi:10.3390/ma13092067
- 626 42. Rouison D, Sain M, Couturier M. Resin transfer molding of hemp fiber composites:
627 optimization of the process and mechanical properties of the materials. *Compos Sci*
628 *Technol.* 2006;66(7-8):895-906. doi:10.1016/j.compscitech.2005.07.040
- 629 43. Ho M po, Lau K tak, Wang H, Hui D. Improvement on the properties of polylactic
630 acid (PLA) using bamboo charcoal particles. *Compos Part B Eng.* 2015;81:14-25.
631 doi:10.1016/j.compositesb.2015.05.048
- 632 44. Sreekumar PA, Joseph K, Unnikrishnan G, Thomas S. A comparative study on
633 mechanical properties of sisal-leaf fibre-reinforced polyester composites prepared
634 by resin transfer and compression moulding techniques. *Compos Sci Technol.*
635 2007;67(3-4):453-461. doi:10.1016/j.compscitech.2006.08.025
- 636 45. Xiao X, Chevali VS, Song P, He D, Wang H. Polylactide/hemp hurd biocomposites
637 as sustainable 3D printing feedstock. *Compos Sci Technol.* 2019;184:107887.
638 doi:10.1016/j.compscitech.2019.107887
- 639 46. Dash BN, Nakamura M, Sahoo S, Kotaki M, Nakai A, Hamada H. Mechanical
640 Properties of Hemp Reinforced Poly(butylene succinate) Biocomposites. *J Biobased*
641 *Mater Bioenergy.* 2008;2(3):273-281. doi:10.1166/jbmb.2008.403
- 642 47. Dolza C, Gongga E, Fages E, Tejada-Oliveros R, Balart R, Quiles-Carrillo L. Green
643 Composites from Partially Bio-Based Poly(butylene succinate-co-adipate)-PBSA
644 and Short Hemp Fibers with Itaconic Acid-Derived Compatibilizers and
645 Plasticizers. *Polymers.* 2022;14(10):1968. doi:10.3390/polym14101968

- 646 48. Qu J ping, Tan B, Feng Y hong, Hu S xi. Mechanical Properties of Poly(Butylene
647 Succinate) Reinforced with Continuously Steam-Exploded Cotton Stalk Bast.
648 *Polym-Plast Technol Eng.* 2011;50(14):1405-1411.
649 doi:10.1080/03602559.2011.593081
- 650 49. Muthuraj R, Misra M, Mohanty AK. Biodegradable biocomposites from
651 poly(butylene adipate- *co* -terephthalate) and miscanthus: Preparation,
652 compatibilization, and performance evaluation. *J Appl Polym Sci.*
653 2017;134(43):45448. doi:10.1002/app.45448
- 654 50. Graupner N. Improvement of the Mechanical Properties of Biodegradable Hemp
655 Fiber Reinforced Poly(lactic acid) (PLA) Composites by the Admixture of Man-
656 made Cellulose Fibers. *J Compos Mater.* 2009;43(6):689-702.
657 doi:10.1177/0021998308100688

658